

# PACER: Blockwise Pre-verification for Speculative Decoding with Adaptive Length

Situo Zhang<sup>1\*</sup>, Yifan Zhang<sup>1\*</sup>, Zichen Zhu<sup>1</sup>, Hankun Wang<sup>1</sup>, Da Ma<sup>1</sup>,  
 Danyang Zhang<sup>1</sup>, Lu Chen<sup>1,2,3</sup>, Kai Yu<sup>1,2,3</sup>

<sup>1</sup>X-LANCE Lab, School of Computer Science  
 MoE Key Lab of Artificial Intelligence, SJTU AI Institute  
 Shanghai Jiao Tong University, Shanghai, China

<sup>2</sup>Jiangsu Key Lab of Language Computing, Suzhou, China

<sup>3</sup>Suzhou Laboratory, Suzhou, China

## Abstract

Speculative decoding (SD) is a powerful technique for accelerating the inference process of large language models (LLMs) without sacrificing accuracy. Typically, SD employs a small draft model to generate a fixed number of draft tokens, which are then verified in parallel by the target model. However, our experiments reveal that the optimal draft length varies significantly across different decoding steps. This variation suggests that using a fixed draft length limits the potential for further improvements in decoding speed. To address this challenge, we propose PACER, a novel approach that dynamically controls draft length using a lightweight, trainable pre-verification layer. This layer pre-verifies draft tokens blockwise before they are sent to the target model, allowing the draft model to stop token generation if the blockwise pre-verification fails. We implement PACER on multiple SD model pairs and evaluate its performance across various benchmarks. Our results demonstrate that PACER achieves up to  $2.66 \times$  Speedup over autoregressive decoding and consistently outperforms standard speculative decoding. Furthermore, when integrated with Ouroboros, PACER attains up to  $3.09 \times$  Speedup.

## 1 Introduction

Large language models (LLMs) have revolutionized artificial intelligence in recent years Achiam et al. (2023); Guo et al. (2025); Yang et al. (2025), demonstrating exceptional capabilities across a wide range of tasks, including conversational agents Chiang et al. (2024), code generation Jimenez et al. (2024), and complex reasoning Luong et al. (2025). Despite their impressive performance, the autoregressive nature of current LLMs, which generate tokens sequentially, introduces substantial inference latency. This latency is primarily caused by memory bandwidth constraints (**memory bound**) rather than computational limitations (**compute bound**) Shazeer (2019); Cai et al. (2024), leading to underutilization of GPU parallelism. As a result, LLMs remain difficult to deploy in time-critical applications and on resource-constrained edge devices Stern et al. (2018); Ivanov et al. (2021).

Numerous methods have been proposed to address this challenge, among which speculative decoding (SD) stands out as an effective technique for accelerating LLM inference Stern et al. (2018); Leviathan et al. (2023); Chen et al. (2023). The core idea involves splitting the decoding process into two stages: drafting and verification. A small and efficient draft model predicts a sequence of  $\gamma$  tokens in advance, which are then verified in a single forward pass by the larger target model. This approach preserves the quality of the generated output while improving inference speed.

---

\*Equal contribution.

Most existing approaches employ a fixed number of draft tokens, denoted as  $\gamma$  (also referred to as the *window size*), throughout the entire decoding process. This window size is typically determined manually by testing various values to achieve the best Speedup in experiments. However, we observe that the acceptance length varies significantly across different decoding steps, as illustrated in Figure 2(a). This variation indicates that using a fixed window size often leads to suboptimal drafting behavior. The limitations of fixed window sizes are twofold: (1) overly conservative window size (small  $\gamma$ ) results in unnecessary target model verification overhead (Figure 1(b)), while (2) excessively large windows (large  $\gamma$ ) waste computation on ultimately rejected drafts (Figure 1(c)). Our preliminary experiments show that dynamically setting the optimal window size for each decoding step can improve overall throughput by up to  $1.4\times$  compared to using a fixed window size, as shown in Figure 2(b). These findings highlight the need for an effective and efficient method to dynamically determine the optimal draft window size at each decoding step.

Several works have attempted to address this challenge by leveraging inherent outputs of draft models, such as token probabilities or entropy, to estimate token acceptance rates [Joao Gante \(2023\)](#); [Brown et al. \(2024\)](#); [Wang et al. \(2025\)](#); [Agrawal et al. \(2024\)](#); [Zhang et al. \(2024b\)](#). While these metrics reflect the model’s semantic uncertainty to some extent, studies have shown that their accuracy often fluctuates with task and data distribution changes, making it difficult to ensure robust and consistent performance [Valentin et al. \(2024\)](#). Additionally, LLMs are prone to miscalibration, particularly in the form of overconfidence [Quevedo et al. \(2024\)](#); [Valentin et al. \(2024\)](#). Relying solely on these metrics overlooks the generated context and its alignment with the target model, leading to naive and unreliable acceptance rate estimates. On the other hand, PEARL [Liu et al. \(2025\)](#) proposes a framework that runs the draft and target models in parallel. However, this approach struggles to efficiently schedule GPU resources in low-resource scenarios, particularly when both models are colocated on the same device. They compete for computational resources, ultimately slowing down execution. Additionally, PEARL requires the draft model’s total inference cost per step to be of the same order of magnitude as the target model’s, which limits its practicality.

To address this issue, we propose PACER, a decoding framework that uses a trainable blockwise pre-verification module to dynamically regulate the draft window size during speculative decoding based on contextual information. Specifically, PACER pre-verifies whether draft tokens are likely to be accepted before they are formally verified by the target model. As shown in Figure 1(a), the draft model first generates tokens in blocks of size  $b$ , and a pre-verification layer is then introduced to pre-verify each block of  $b$  tokens. If the tokens in the current block pass the pre-verification, the draft model continues to generate the next  $b$ -token block; otherwise, it stops. This approach minimizes the misclassification of individual draft tokens and amortizes the additional inference overhead introduced by the pre-verification module. Furthermore, PACER incorporates positional encoding for draft tokens, enabling more accurate predictions of acceptance probabilities and better optimization of dynamic window sizes.

We implement PACER on multiple SD model pairs, including DeepSeek-Coder [Guo et al. \(2024\)](#), Llama-2 [Touvron et al. \(2023\)](#), and Qwen-2.5 [Yang et al. \(2024\)](#), and evaluate its performance across various text generation benchmarks, such as code generation [Chen et al. \(2021\)](#), mathematical reasoning [Cobbe et al. \(2021\)](#), and text summarization [See et al. \(2017\)](#). Experimental results demonstrate that PACER achieves up to  $2.66\times$  Speedup over vanilla autoregressive decoding and consistently outperforms SD with a fixed window size. Moreover, when integrated with Ouroboros, PACER achieves up to  $3.09\times$  Speedup over autoregressive decoding. In summary, our main contributions are as follows:

- We present a systematic analysis of the performance gains enabled by adaptive draft lengths and provide key empirical insights that directly motivate the design of our dynamic draft-length framework.
- We propose PACER, an effective and efficient framework that dynamically controls and leads to an optimal draft window size by pre-verifying draft tokens blockwise and leveraging draft position information.

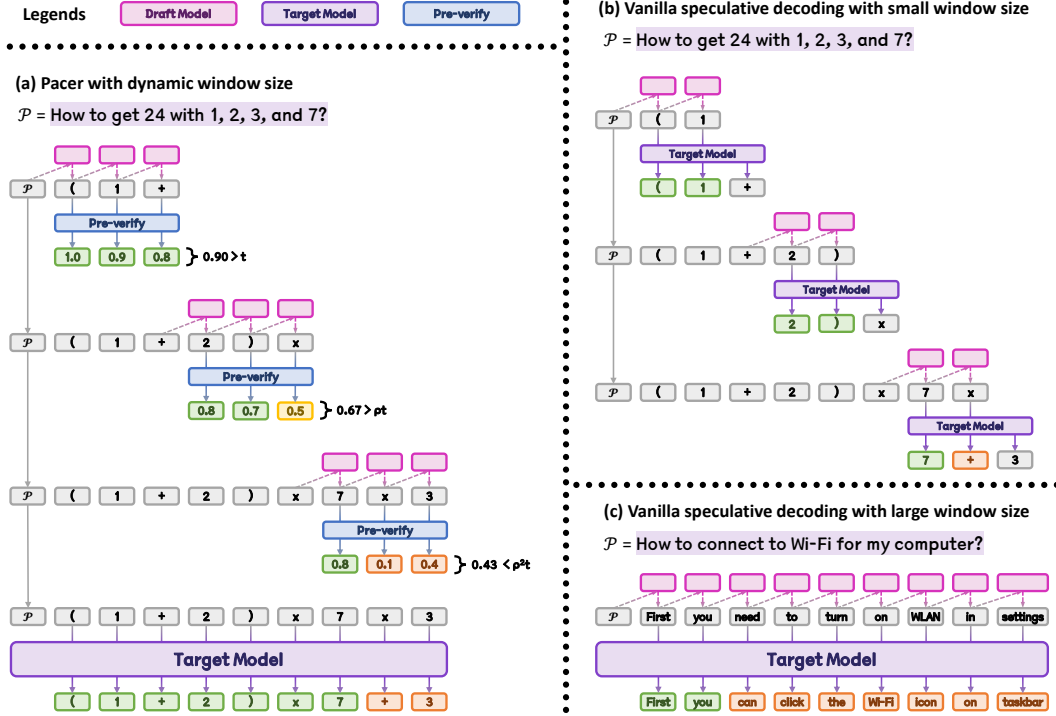


Figure 1: Comparison of the speculative decoding (SD) process for PACER and vanilla SD with fixed small and large window sizes. (a) PACER generates drafts in blocks of size  $b = 3$ , performs three rounds of pre-verification, and produces a total of **9** draft tokens, of which **7** are accepted with only **one** target model forward pass. (b) Vanilla SD with a small window size ( $\gamma = 2$ ) causes the draft model to stop prematurely, resulting in **3 costly** target forward and **6** draft forward. (c) Vanilla SD with a large window size  $\gamma = 9$  generates **9** draft tokens, but only **2** are accepted, leading to wasted draft computation.

- We conduct extensive evaluations of PACER on multiple text generation benchmarks, demonstrating its effectiveness in consistently outperforming baseline methods and speculative decoding approaches with fixed window sizes.
- We further show that PACER is compatible with other speculative decoding methods designed to improve draft generation quality, and can be seamlessly integrated with such techniques to achieve additional performance gains, validating the universality of our approach.

## 2 Preliminary

### 2.1 Notations

In this paper, we denote the target model by  $M_T$ , the draft model by  $M_D$ , and our blockwise pre-verification layer by  $M_B$ . Let  $\mathcal{V}$  represent the vocabulary set with size  $V$ , and let  $\gamma$  denote the window size, i.e., the number of draft tokens generated by  $M_D$  before verification by  $M_T$ . Given an input prefix sequence  $\mathbf{x} = [x_1, x_2, \dots, x_n]$  of length  $n$ , we define the autoregressive generation of  $m$  tokens using model  $M$  as:

$$(y_1, p_1), (y_2, p_2), \dots, (y_m, p_m) = M^m(\mathbf{x}), \quad (1)$$

where  $y_1, \dots, y_m \in \mathcal{V}$  are the generated tokens, and  $p_1, \dots, p_m \in \mathbb{R}^V$  are their corresponding decoding distributions. Each draft token  $y_i$  is sampled according to its distribution,  $y_i \sim p_i$ , for  $i = 1, \dots, m$ .

For a parallel forward pass of model  $M$ , we have:

$$p_1, \dots, p_{m+1} = M(y_1, \dots, y_m; \mathbf{x}), \quad (2)$$

where  $p_{m+1}$  denotes the distribution for the next token after  $y_m$ .

## 2.2 Speculative Decoding

Speculative decoding consists of two stages: drafting and verification. Given an input prefix  $\mathbf{x}$ , the draft model first autoregressively generates  $\gamma$  draft tokens:

$$(y_1, q_1), \dots, (y_\gamma, q_\gamma) = M_D^\gamma(\mathbf{x}), \quad (3)$$

where  $q_1, \dots, q_\gamma$  denote the candidate distributions. Subsequently, the target model verifies the drafts  $y_1, \dots, y_\gamma$  by performing a parallel forward pass with the concatenated prefix  $\mathbf{x}$ :

$$p_1, \dots, p_{\gamma+1} = M_T(y_1, \dots, y_\gamma; \mathbf{x}). \quad (4)$$

The acceptance rate of each draft token  $y_i$  is calculated as:

$$\alpha_i = \begin{cases} 1, & \text{if } p_i[y_i] \geq q_i[y_i], \\ \frac{p_i[y_i]}{q_i[y_i]}, & \text{otherwise.} \end{cases} \quad (5)$$

If token  $y_i$  is rejected, all subsequent tokens  $y_{i+1}, \dots, y_\gamma$  are discarded, and a new token is resampled from the normalized distribution  $\text{norm}(\max(0, p_i - q_i))$ . If all drafts are accepted, SD samples an additional token from distribution  $p_{\gamma+1}$ . This process allows SD to validate multiple tokens in one parallel step, substantially reducing the sequential steps required in autoregressive decoding. Importantly, the resulting output distribution remains consistent with that of vanilla autoregressive decoding of the target LLM [Leviathan et al. \(2023\)](#).

## 2.3 Acceptance Length

The acceptance length  $L_A$  denotes the number of draft tokens accepted in a single SD step, which includes both the drafting and verification phases. It is bounded by the draft window size  $\gamma$ , such that  $0 \leq L_A \leq \gamma$ . The value of  $L_A$  is jointly determined by the draft model and the target model, reflecting how well the draft model fits the target model's next-token distribution.

A larger fixed window size typically yields a longer acceptance length, but it also increases the number of draft tokens that may be rejected, leading to wasted draft-model computation. Conversely, a smaller fixed window size reduces draft waste but limits the attainable acceptance length, resulting in more frequent and costly target-model forward passes. These trade-offs highlight the importance of employing a dynamic window size that adapts to the acceptance behavior observed during decoding.

## 3 Method

In this section, we first present observations on acceptance lengths across decoding steps and demonstrate the speedup achieved by using optimal draft lengths. We then introduce PACER, a decoding framework that dynamically controls the draft window size by pre-verifying draft tokens in a blockwise manner. Finally, we describe the training of PACER.

### 3.1 Observations

#### 3.1.1 Acceptance Lengths Vary Significantly Between Steps

We conduct pilot experiments using DeepSeek-Coder models [Guo et al. \(2024\)](#), employing the 1.3B model as the draft model and the 33B model as the target model on HumanEval [Chen et al. \(2021\)](#). To obtain the maximum acceptance lengths  $L_A^*$ , we set the draft

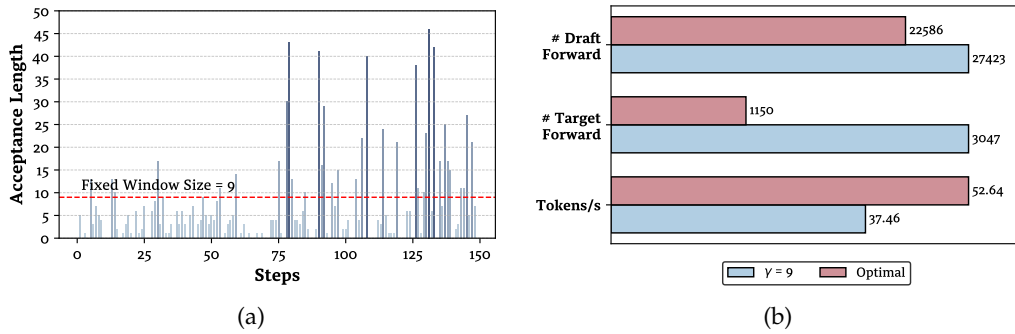


Figure 2: (a) Maximum acceptance lengths across decoding steps. The optimal fixed window size ( $\gamma = 9$ ) is marked by the red horizontal line. Significant variation in acceptance lengths highlights the inefficiency of employing a fixed draft window size. (b) Comparison between speculative decoding using the optimal fixed window ( $\gamma = 9$ ) and optimal dynamic window size ( $\gamma^*$ ). Utilizing dynamic draft lengths substantially reduces forward passes for both draft and target models, leading to increased decoding speed (tokens/s).

window size sufficiently large during decoding. The acceptance lengths across different decoding steps are plotted in Figure 2(a).

Our analysis reveals significant variation in acceptance lengths between decoding steps, demonstrating the suboptimality of fixed window sizes. This manifests in two key inefficiencies:

1. When  $\gamma > L_A^*$ , particularly when  $L_A^* \approx 0$ , computation resources are wasted on generating ultimately rejected draft tokens.
2. When  $\gamma < L_A^*$  (the bars with long acceptance lengths in Figure 2(a)), the draft model prematurely terminates, missing opportunities to generate additional accepted tokens. This results in unnecessary target model forward passes, which are computationally expensive.

Thus, dynamically adjusting the window size is essential for optimizing the efficiency of speculative decoding.

### 3.1.2 Optimal Draft Lengths Enhance SD Efficiency

We define the optimal draft length  $\gamma^*$  as the maximum acceptance length  $L_A^*$  for each decoding step. As illustrated in Figure 2(b), compared to the best-performing SD method with a fixed window size 9, SD using  $\gamma^*$  reduces the number of draft forward passes by 4,837, and significantly decreases target forward passes from 3,047 to 1,150, resulting in an overall Speedup of  $1.4\times$ . This improvement arises from minimizing computational overhead associated with redundant forward passes in both draft and target models. Thus, accurately estimating  $\gamma^*$  can significantly enhance the efficiency of SD.

### 3.1.3 Acceptance Rates Decrease with Draft Position

We analyze how the acceptance rate varies with the position of a draft token and visualize this trend in Figure 6. The results show a sharp decline in acceptance rates as the draft position increases, indicating that tokens appearing later in the draft sequence are substantially less likely to be accepted by the target model. This suggests that it is possible to incorporate positional information when predicting acceptance probabilities.

## 3.2 PACER

Based on the observations in Section 3.1, we note that acceptance length strongly depends on the generated context. Therefore, we introduce PACER, a trainable module designed to

leverage draft contexts to approximately pre-verify draft tokens in a blockwise manner. The workflow of PACER is illustrated in Figure 1(a). To achieve a balance between prediction accuracy and computational overhead, PACER employs a single-layer Transformer atop the draft model to capture context and perform pre-verification predictions blockwise.

Our key insight is that accurately predicting draft acceptance rates requires considering all prior draft context. However, we observe that the forward-pass latency of the pre-verification layer is non-negligible. To balance accuracy and computational efficiency, we perform pre-verification in blocks of size  $b$ , effectively amortizing this overhead. Specifically, given a prefix  $\mathbf{x}$ , the draft model  $M_D$  begins by generating  $b$  draft tokens:

$$(y_1, h_1), \dots, (y_b, h_b) = M_D^b(\mathbf{x}), \quad (6)$$

where  $h_1, \dots, h_b$  represent the hidden states of the  $b$  drafts. The pre-verification layer  $M_B$  then processes these hidden states along with positional embeddings:

$$\hat{\alpha}_1, \dots, \hat{\alpha}_b = M_B([h_1 + e_1], \dots, [h_b + e_b]; \mathbf{h}_x), \quad (7)$$

Here,  $\hat{\alpha}_1, \dots, \hat{\alpha}_b$  represent the estimated acceptance rates for drafts  $y_1, \dots, y_b$ , while  $e_1, \dots, e_b$  denote positional embeddings corresponding to draft positions 1 to  $b$ . Additionally,  $\mathbf{h}_x$  represents the hidden states of previously accepted tokens before the current draft-and-verify step. We compute the mean estimated acceptance rate across the block,  $\text{mean}(\hat{\alpha}_1, \dots, \hat{\alpha}_b)$ , and stop drafting if this mean falls below a predefined threshold  $t$ , triggering verification by the target model  $M_T$ . Otherwise,  $M_D$  continues to generate another block of  $b$  tokens. For next pre-verification rounds, the draft positions become  $b+1, \dots, 2b$ , and so forth. For drafts with  $k$  pre-verification rounds, the final window size for that decoding step is  $\gamma = k \cdot b$ . Meanwhile, the threshold  $t$  is increased each round by a growth factor  $\rho > 1$ , making it progressively easier to stop draft generation in later steps. The detailed algorithm is presented in Section A.

### 3.3 Training

To ensure consistency between training and inference, we first utilize the target model  $M_T$  to generate responses based on instructions from the training datasets. We then apply the same speculative decoding process used during inference to construct labeled acceptance data. Specifically, the draft model  $M_D$  starts from a given prefix sequence  $\mathbf{x}$  and generates a sequence of draft tokens  $y_1, \dots, y_\gamma$  using a large window size (e.g.,  $\gamma = 50$ ). We compare these drafts against tokens generated by the target model: if a draft token  $y_i$  differs from the corresponding target token, all subsequent tokens  $y_i, \dots, y_\gamma$  are labeled as 0 (rejected), while tokens  $y_1, \dots, y_{i-1}$  are labeled as 1 (accepted). This procedure produces labeled training data aligned precisely with the inference-time verification process. We train the pre-verification layer  $M_B$  using standard cross-entropy loss. To improve training efficiency, we pack draft tokens from multiple decoding steps into a single sequence with carefully designed attention masks. Further details about training are provided in Section D.

## 4 Experiments

### 4.1 Experiments Setting

**Evaluation Datasets.** We evaluate PACER on multiple representative text-generation benchmarks to demonstrate its effectiveness. Specifically, for code generation tasks, we utilize two widely adopted benchmarks: HumanEval (Chen et al., 2021) and MBPP (Austin et al., 2021). For document summarization, we employ the well-established CNN/Daily Mail (CNN/DM) dataset (See et al., 2017). Additionally, for arithmetic reasoning, we use the GSM8K dataset (Cobbe et al., 2021). Further details on evaluation datasets can be found in Section C.1.

**Training Datasets.** We use the CodeAlpaca dataset (Chaudhary, 2023), which contains approximately 20,000 instruction-response pairs covering a wide range of programming scenarios and coding tasks. We use the instructions to generate our training data.

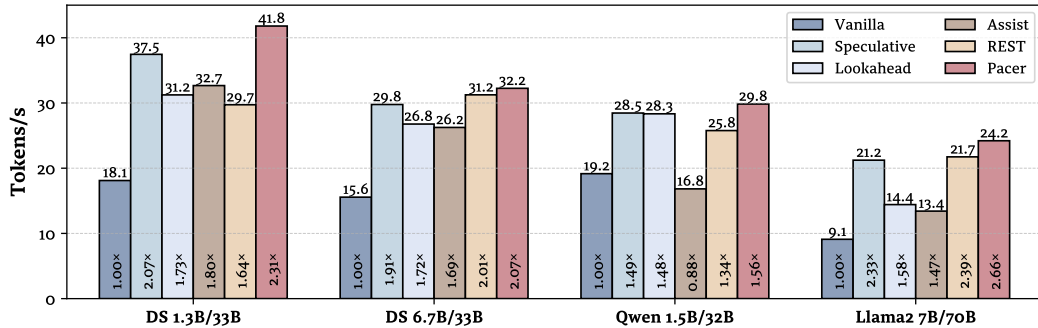


Figure 3: Comparison of decoding speeds (tokens/s) and speedup for different methods on the HumanEval dataset. PACER consistently outperforms all baseline methods across various models.

**Models.** We employ several state-of-the-art LLMs widely used in current research, including the DeepSeek-Coder series (Guo et al., 2024), the Llama2 series (Touvron et al., 2023), and the Qwen2.5 series (Yang et al., 2024). Specifically, we adopt **1.3B/33B** and **6.7B/33B** models from the DeepSeek-Coder series, **7B/70B** models from the Llama2-chat series, and **1.5B/32B** models from the Qwen2.5 series, using less-parameter models as drafts and their larger counterparts as target models. These models encompass a wide range of model sizes representative of LLM research.

**Evaluation Methods.** We compare our method against several established baselines, including vanilla autoregressive decoding, speculative decoding (Leviathan et al., 2023; Chen et al., 2023), lookahead decoding (Fu et al., 2024), a heuristic-based dynamic window method (assist generation) (Joao Gante, 2023), and retrieval-based decoding (REST) (He et al., 2024). To ensure fair comparisons on our hardware setup, we reproduced each baseline using their official implementations and default parameters. In all experiments, including both baselines and our proposed method, we set the batch size to 1, which is standard across speculative decoding frameworks. We evaluate model performance using the following metrics: **decoding speed (tokens/s)**, **speedup ratio**, and **average acceptance lengths ( $\tau$ )**. The detailed evaluation settings can be found in Section C.1.

## 4.2 Main Results

We conducted experiments on the benchmarks described previously. As shown in Figure 3, PACER consistently outperformed vanilla autoregressive decoding, speculative decoding, lookahead decoding, assist generation, and REST across all evaluated model series on the HumanEval dataset. Specifically, in experiments using DeepSeek-Coder 1.3B/33B, PACER achieved a decoding speed of 41.8 tokens/s, corresponding to a 2.31 $\times$  speedup over vanilla autoregressive decoding and surpassing the 2.07 $\times$  speedup achieved by vanilla speculative decoding. For Llama-2 7B/70B, the speedup improved from 2.33 $\times$  to 2.66 $\times$ . Table 1 further presents decoding speeds and corresponding speedup ratios for various methods across multiple datasets. PACER consistently achieved the highest decoding speeds and speedups across all models, outperforming all tested methods. Notably, on the GSM8K dataset, the speedup ratio improved from 1.92 $\times$  to 2.17 $\times$  with DeepSeek-Coder 1.3B/33B and from 1.94 $\times$  to 2.08 $\times$  with Llama-2 7B/70B. These results demonstrate that utilizing a blockwise pre-verification layer to dynamically control draft lengths effectively leverages the capabilities of the draft model, yielding significant performance improvements across diverse tasks and model setups.

## 4.3 Comparison with Other Dynamic Draft Length Methods

We benchmark PACER against several state-of-the-art methods that utilize dynamic draft lengths, including AdaEDL (Agrawal et al., 2024), which generates drafts based on the

Algorithm	Deepseek 1.3B/33B		Deepseek 6.7B/33B		Llama-2 7B/70B	
	tokens/s	speedup	tokens/s	speedup	tokens/s	speedup
<i>MBPP</i>						
Vanilla	17.53	1.00	15.86	1.00	9.28	1.00
Speculative	30.72	1.75	26.62	1.68	18.65	2.01
Lookahead	29.55	1.69	23.67	1.49	13.30	1.43
Assist	26.60	1.52	21.07	1.33	16.30	1.76
REST	29.41	1.69	25.64	1.60	15.38	1.66
PACER	<b>32.93</b>	<b>1.88</b>	<b>28.57</b>	<b>1.80</b>	<b>19.90</b>	<b>2.14</b>
<i>CNN/DM</i>						
Vanilla	17.11	1.00	15.37	1.00	8.46	1.00
Speculative	23.55	1.38	20.55	1.34	14.40	1.70
Lookahead	18.21	1.08	17.64	1.15	8.56	1.01
Assist	22.27	1.30	18.52	1.20	11.36	1.34
REST	18.50	1.06	16.70	1.09	9.62	1.14
PACER	<b>23.77</b>	<b>1.39</b>	<b>21.51</b>	<b>1.40</b>	<b>14.50</b>	<b>1.71</b>
<i>GSM8k</i>						
Vanilla	18.25	1.00	16.51	1.00	9.19	1.00
Speculative	35.08	1.92	29.36	1.78	17.81	1.94
Lookahead	33.82	1.85	29.09	1.76	12.07	1.31
Assist	34.86	1.91	28.80	1.74	14.02	1.53
REST	23.25	1.27	22.22	1.34	12.66	1.38
PACER	<b>39.69</b>	<b>2.17</b>	<b>31.07</b>	<b>1.88</b>	<b>19.07</b>	<b>2.08</b>

Table 1: Decoding speed (tokens/s) and speedup across different methods and LLM families on MBPP, CNN/DM and GSM8K benchmarks.

Method	MT-Bench	Translation	Summarization	QA	Math Reasoning	RAG	Average
Vanilla	9.04	9.31	8.63	9.32	9.29	8.32	8.99
Assist	17.77	17.95	16.42	17.10	20.46	15.60	17.58
AdaEDL	17.55	17.85	16.10	17.34	20.21	15.69	17.47
SpecDec++	18.18	17.62	<b>16.57</b>	17.41	20.81	<b>15.80</b>	17.79
PACER	<b>18.53</b>	<b>18.06</b>	16.19	<b>17.42</b>	<b>21.45</b>	15.48	<b>17.95</b>

Table 2: Decoding speed (tokens/s) on SpecBench with Llama-2 7B/70B.

entropy of draft token distributions, and SpecDec++ (Huang et al., 2024), which controls draft lengths using an additional prediction head. We conduct a focused comparison on the HumanEval benchmark. As shown in Table 3, PACER outperforms all other dynamic methods, achieving the highest decoding speed (24.20 tokens/s) and significantly longer average acceptance length (7.46). These results highlight the effectiveness of our pre-verification layer.

Additionally, we evaluate these methods on the SpecBench benchmark (Xia et al., 2024a). As shown in Table 2, PACER consistently achieves the highest average decoding speed, confirming the generalizability of our pre-verification mechanism.

#### 4.4 Integration with Ouroboros

To demonstrate the flexibility and orthogonality of PACER, we integrated it with Ouroboros (Zhao et al., 2024), a recent method that improves drafting efficiency by generating phrase-level drafts from an n-gram pool. While Ouroboros enhances draft quality, it employs a fixed draft steps. In contrast, PACER dynamically adjusts draft lengths via pre-verification. We hypothesized that combining these complementary strategies could yield further performance improvements. We conducted experiments on the HumanEval, MBPP, and GSM8K benchmarks using DeepSeek-Coder 1.3B/33B, using the optimal configuration from the Ouroboros paper.

Method	tokens/s	$\tau$
Speculative	21.20	5.39
SpecDec++*	21.17	5.13
AdaEDL	22.53	4.57
PACER	<b>24.20</b>	<b>7.46</b>

Table 3: Decoding speed (tokens/s) and average acceptance length ( $\tau$ ) of dynamic draft length methods on HumanEval with Llama-2 7B/70B. \*SpecDec++ underperforms standard SD here due to differences in chat templates compared to its original paper. We present results obtained using the original SpecDec++ templates in the appendix, where PACER remains superior.

Dataset	Method	tokens/s	speedup	$\tau$
<i>HumanEval</i>	Vanilla	18.10	1.00	—
	Ouroboros	49.05	2.71	8.36
	PACER + Ouroboros	<b>51.07</b>	<b>2.82</b>	<b>10.90</b>
<i>MBPP</i>	Vanilla	17.53	1.00	—
	Ouroboros	47.99	2.74	3.81
	PACER + Ouroboros	<b>50.08</b>	<b>2.86</b>	<b>5.10</b>
<i>GSM8K</i>	Vanilla	18.25	1.00	—
	Ouroboros	52.66	2.89	4.43
	PACER + Ouroboros	<b>56.31</b>	<b>3.09</b>	<b>5.99</b>

Table 4: Comparison of decoding speed (tokens/s) and the average acceptance lengths ( $\tau$ ) on benchmark HumanEval, MBPP, and GSM8K using Deepseek-Coder 1.3B/33B, when combining PACER with Ouroboros.

As shown in Table 4, the integrated approach consistently achieves higher decoding speeds and longer average acceptance lengths. For example, on GSM8K, the speedup increases from  $2.89 \times$  with Ouroboros alone to  $3.09 \times$  with the combined method. These findings highlight the adaptability of PACER and its effectiveness in enhancing other SD methods that optimize the draft process.

#### 4.5 Ablation Studies

Method	HumanEval			GSM8K		
	tokens/s	speedup	$\tau$	tokens/s	speedup	$\tau$
Vanilla	18.11	1.00	—	18.25	1.00	—
Speculative	37.46	2.07	7.38	35.08	1.94	5.87
PACER	<b>41.80</b>	<b>2.31</b>	9.67	<b>39.69</b>	<b>2.17</b>	7.23
w/o pos-emb	39.99	2.21	8.83	37.48	2.05	7.19
w/o growth-factor	40.36	2.23	<b>9.71</b>	37.84	2.07	<b>7.46</b>

Table 5: Ablations on draft position embedding and threshold growth factor with DeepSeek-Coder 1.3B/33B.

We conduct a series of ablation studies to examine the key components of our approach. Specifically, we analyze the impact of draft position embeddings (**pos-emb**) and the threshold growth factor (**growth-factor**) on overall performance. We also carried out additional ablations to analyze our hyperparameter settings and key aspects of our model design. Additional ablations are presented in appendix.

**Effect of Position Embedding.** As shown in Table 5, removing draft position embeddings reduces the decoding speed to 39.99 tokens/s, indicating that position information contributes significantly to the overall performance of PACER. This aligns with the observation that

draft position serves as a strong indicator of acceptance rate, and incorporating it enhances prediction accuracy.

**Effect of Growth Factor.** As shown in Table 5, removing the threshold growth factor increases the average acceptance length  $\tau$ , but results in lower decoding speed. This indicates that the growth factor plays a crucial role by progressively increasing the likelihood of early stopping as draft sequences grow longer. Without it, PACER tends to generate overly long drafts, leading to wasted computation and reduced efficiency.

## 5 Discussion

In this section, we investigate the underlying factors that enable PACER to accelerate speculative decoding and discuss key architectural design choices. We analyze the performance contributions of PACER, examine alternative halting criteria for draft generation, and evaluate the impact of different attention scopes in the pre-verification layer.

### 5.1 Where Does the Speedup of PACER Come From?

To understand the performance advantages of PACER, we record the number of forward passes for both the draft and target models, along with the average acceptance length. As shown in Table 6, PACER with DeepSeek-Coder 1.3B/33B achieves substantial improvements over speculative decoding with the optimal fixed window size across HumanEval, CNN/DM, and GSM8K. PACER reduces the forward passes for both the draft and target models while simultaneously increasing the average acceptance length.

These improvements arise from PACER’s ability to adaptively adjust the draft window size. It halts early in regions where predictions are uncertain, preventing wasted draft computation, and produces longer drafts in segments where acceptance likelihood is high. This adaptive behavior improves data-movement efficiency, alleviates the memory bound inherent in autoregressive decoding, and yields consistent speed gains across tasks and model scales.

Methods	HumanEval			CNN/DM			GSM8k		
	#Draft Forward	#Target Forward	$\tau$	#Draft Forward	#Target Forward	$\tau$	#Draft Forward	#Target Forward	$\tau$
Speculative	27423	3047	7.38	23904	7968	1.78	59456	7432	5.87
PACER	<b>26376</b>	<b>2368</b>	<b>9.67</b>	<b>22252</b>	<b>7884</b>	<b>1.89</b>	<b>54024</b>	<b>6816</b>	<b>7.23</b>

Table 6: Comparison of the number of forward passes for the draft and target models, and the average acceptance lengths ( $\tau$ ), between vanilla speculative decoding with optimal fixed window size (Speculative) and PACER across different benchmarks.

### 5.2 What Is the Best Halting Criterion for Draft Generation?

To determine an effective halting criterion for the pre-verification stage, we compare our proposed mean-token probability criterion with two stricter alternatives: (1) **Any-token below  $t$** : stopping when **any** token in the block has predicted acceptance below threshold  $t$ , and (2) **Last-token below  $t$** : stopping based solely on the predicted acceptance of the **last** token in the block. Results are shown in Table 7.

Table 7: Comparison of decoding speed and average acceptance length ( $\tau$ ) using different halting criteria on HumanEval with DeepSeek-Coder 1.3B/33B.

Halting Criterion	Tokens/s	$\tau$
Any-token below $t$	38.96	8.70
Last-token below $t$	40.11	9.34
Mean-token probability $t$ (Ours)	<b>41.80</b>	<b>9.67</b>

As seen in Table 7, our mean-token criterion achieves the highest decoding speed and the longest accepted sequence length. This is because averaging across tokens mitigates the effects of occasional low-confidence predictions. In contrast, stricter criteria tend to halt the draft prematurely, reducing acceptance lengths and lowering overall throughput.

### 5.3 How Does Attention Context Affect Pre-verification?

To validate the importance of full-context attention in the pre-verification layer, we compare it with two restricted variants: (1) **Local block**, where attention is limited to the current block, and (2) **Local draft**, where attention is restricted to the current draft step. Results are summarized in Table 8.

Table 8: Ablation on Attention Context		
Context Scope	Tokens/s	$\tau$
Local block	22.29	5.32
Local draft	22.58	5.45
Full context (Ours)	<b>24.20</b>	<b>7.46</b>

Expanding the attention scope consistently improves decoding speed and acceptance length  $\tau$ . Full-context attention is particularly effective because it captures long-range dependencies within the draft and prefix, enabling more reliable acceptance prediction.

## 6 Related Work

**Speculative Decoding** Speculative decoding (SD) utilizes a draft-verify paradigm to achieve lossless acceleration. Existing SD frameworks can generally be categorized based on the type of draft models used (Xia et al., 2024b). (1) **Independent draft models**: SpecDec (Xia et al., 2023) introduced a non-autoregressive (non-AR) Transformer that generates multiple tokens simultaneously. Several other works (Leviathan et al., 2023; Chen et al., 2023; Spector & Re, 2023; Sun et al., 2023) propose leveraging smaller pretrained models from the same LLM family (e.g., Llama2-7B and Llama2-70B (Touvron et al., 2023)) for inference acceleration, thus avoiding additional training and maintaining alignment in prediction behaviors due to shared tokenizers and training corpora. SpecInfer (Miao et al., 2024) and DistillSpec (Zhou et al., 2024) adopt distillation techniques to obtain smaller draft models. (2) **Self-drafting**: This approach eliminates the need for external draft models by employing the target LLM itself for drafting, thereby ensuring close alignment. Stern et al. (2018); Cai et al. (2024); Hwang et al. (2024); Gloeckle et al. (2024) train multiple heads to simultaneously predict multiple future draft tokens. Eagle (Li et al., 2024b) introduces a single-layer transformer to perform autoregressive prediction at the feature level. Additionally, non-autoregressive decoding methods for generating drafts have been explored by Santilli et al. (2023); Yi et al. (2024); Xiao et al. (2024). Lookahead (Fu et al., 2024) constructs n-gram pools using Jacobi iterations as drafts. Meanwhile, works by Yang et al. (2023); Zhang et al. (2024a); Elhoushi et al. (2024) investigate early exiting and layer skipping within the target model to enhance drafting efficiency. Despite these developments, most approaches utilize fixed window sizes, leaving the challenge of adaptive draft generation largely unaddressed.

**Adaptive Draft Length** Several recent studies have explored the adaptive adjustment of draft lengths. Works by Zhang et al. (2024a); Liu et al. (2024); Li et al. (2024a); Joao Gante (2023); Brown et al. (2024); Wang et al. (2025); Agrawal et al. (2024); Zhang et al. (2024b) propose determining draft-stopping criteria using intrinsic outputs from draft models, such as token probability or entropy, to estimate draft acceptance rates. These methods typically rely on manually set thresholds or update rules to establish when to stop drafting. Although heuristic-based approaches offer simplicity and computational efficiency, relying solely on semantic uncertainty metrics lacks robustness and consistent accuracy. This is primarily due to the inherent miscalibration and overconfidence exhibited by LLMs (Quevedo et al., 2024; Valentin et al., 2024; Huo et al., 2025), resulting in overly simplistic and unreliable estimations

of acceptance rates. SpecDec++ (Huang et al., 2024) and DISCO (Mamou et al., 2024) address this by training classifiers on top of draft models to determine when to stop token generation, but they neglect draft-context information. Meanwhile, PEARL (Liu et al., 2025) introduces a parallel framework allowing concurrent operation of target and draft models; however, it faces challenges handling resource constraints due to competition when both models are colocated. To address these limitations, we propose PACER, a decoding framework that leverages a trainable blockwise pre-verification layer incorporating contextual information to efficiently and accurately determine the optimal draft length.

## 7 Conclusion

In this paper, we propose PACER, an effective and efficient approach that dynamically controls draft lengths based on contextual information. PACER employs a trainable pre-verification layer to blockwise pre-verify draft tokens. The draft model continues generating tokens only when the block passes pre-verification. This adaptive strategy effectively mitigates computational waste associated with fixed window sizes in speculative decoding. We conduct comprehensive experiments across diverse benchmarks, and PACER consistently outperforms all speculative decoding baselines across model architectures, demonstrating its effectiveness in handling variable draft lengths.

## References

Josh Achiam, Steven Adler, Sandhini Agarwal, Lama Ahmad, Ilge Akkaya, Florencia Leoni Aleman, Diogo Almeida, Janko Altenschmidt, Sam Altman, Shyamal Anadkat, et al. Gpt-4 technical report. *arXiv preprint arXiv:2303.08774*, 2023.

Sudhanshu Agrawal, Wonseok Jeon, and Mingu Lee. Adaedl: Early draft stopping for speculative decoding of large language models via an entropy-based lower bound on token acceptance probability. In *NeurIPS Efficient Natural Language and Speech Processing Workshop*, pp. 355–369. PMLR, 2024.

Jacob Austin, Augustus Odena, Maxwell Nye, Maarten Bosma, Henryk Michalewski, David Dohan, Ellen Jiang, Carrie Cai, Michael Terry, Quoc Le, et al. Program synthesis with large language models. *arXiv preprint arXiv:2108.07732*, 2021.

Oscar Brown, Zhengjie Wang, Andrea Do, Nikhil Mathew, and Cheng Yu. Dynamic depth decoding: Faster speculative decoding for llms, 2024. URL <https://arxiv.org/abs/2409.00142>.

Tianle Cai, Yuhong Li, Zhengyang Geng, Hongwu Peng, Jason D. Lee, Deming Chen, and Tri Dao. Medusa: Simple LLM inference acceleration framework with multiple decoding heads. In Ruslan Salakhutdinov, Zico Kolter, Katherine Heller, Adrian Weller, Nuria Oliver, Jonathan Scarlett, and Felix Berkenkamp (eds.), *Proceedings of the 41st International Conference on Machine Learning*, volume 235 of *Proceedings of Machine Learning Research*, pp. 5209–5235. PMLR, 21–27 Jul 2024. URL <https://proceedings.mlr.press/v235/cai24b.html>.

Sahil Chaudhary. Code alpaca: An instruction-following llama model for code generation. <https://github.com/sahil280114/codealpaca>, 2023.

Charlie Chen, Sebastian Borgeaud, Geoffrey Irving, Jean-Baptiste Lespiau, Laurent Sifre, and John Jumper. Accelerating large language model decoding with speculative sampling, 2023. URL <https://arxiv.org/abs/2302.01318>.

Mark Chen, Jerry Tworek, Heewoo Jun, Qiming Yuan, Henrique Ponde de Oliveira Pinto, Jared Kaplan, Harri Edwards, Yuri Burda, Nicholas Joseph, Greg Brockman, Alex Ray, Raul Puri, Gretchen Krueger, Michael Petrov, Heidy Khlaaf, Girish Sastry, Pamela Mishkin, Brooke Chan, Scott Gray, Nick Ryder, Mikhail Pavlov, Alethea Power, Lukasz Kaiser, Mohammad Bavarian, Clemens Winter, Philippe Tillet, Felipe Petroski Such, Dave Cummings, Matthias Plappert, Fotios Chantzis, Elizabeth Barnes, Ariel Herbert-Voss, William Hebgen

Guss, Alex Nichol, Alex Paino, Nikolas Tezak, Jie Tang, Igor Babuschkin, Suchir Balaji, Shantanu Jain, William Saunders, Christopher Hesse, Andrew N. Carr, Jan Leike, Josh Achiam, Vedant Misra, Evan Morikawa, Alec Radford, Matthew Knight, Miles Brundage, Mira Murati, Katie Mayer, Peter Welinder, Bob McGrew, Dario Amodei, Sam McCandlish, Ilya Sutskever, and Wojciech Zaremba. Evaluating large language models trained on code, 2021. URL <https://arxiv.org/abs/2107.03374>.

Wei-Lin Chiang, Lianmin Zheng, Ying Sheng, Anastasios Nikolas Angelopoulos, Tianle Li, Dacheng Li, Banghua Zhu, Hao Zhang, Michael Jordan, Joseph E Gonzalez, et al. Chatbot arena: An open platform for evaluating llms by human preference. In *Forty-first International Conference on Machine Learning*, 2024.

Karl Cobbe, Vineet Kosaraju, Mohammad Bavarian, Mark Chen, Heewoo Jun, Lukasz Kaiser, Matthias Plappert, Jerry Tworek, Jacob Hilton, Reiichiro Nakano, Christopher Hesse, and John Schulman. Training verifiers to solve math word problems, 2021. URL <https://arxiv.org/abs/2110.14168>.

Mostafa Elhoushi, Akshat Shrivastava, Diana Liskovich, Basil Hosmer, Bram Wasti, Liangzhen Lai, Anas Mahmoud, Bilge Acun, Saurabh Agarwal, Ahmed Roman, et al. Layerskip: Enabling early exit inference and self-speculative decoding. In *Proceedings of the 62nd Annual Meeting of the Association for Computational Linguistics (Volume 1: Long Papers)*, pp. 12622–12642, 2024.

Yichao Fu, Peter Bailis, Ion Stoica, and Hao Zhang. Break the sequential dependency of llm inference using lookahead decoding. In *International Conference on Machine Learning*, pp. 14060–14079. PMLR, 2024.

Fabian Gloeckle, Badr Youbi Idrissi, Baptiste Rozière, David Lopez-Paz, and Gabriel Synnaeve. Better & faster large language models via multi-token prediction. *arXiv preprint arXiv:2404.19737*, 2024.

Daya Guo, Qihao Zhu, Dejian Yang, Zhenda Xie, Kai Dong, Wentao Zhang, Guanting Chen, Xiao Bi, Yu Wu, YK Li, et al. Deepseek-coder: When the large language model meets programming—the rise of code intelligence. *arXiv preprint arXiv:2401.14196*, 2024.

Daya Guo, Dejian Yang, Haowei Zhang, Junxiao Song, Ruoyu Zhang, Runxin Xu, Qihao Zhu, Shirong Ma, Peiyi Wang, Xiao Bi, et al. Deepseek-r1: Incentivizing reasoning capability in llms via reinforcement learning. *arXiv preprint arXiv:2501.12948*, 2025.

Zhenyu He, Zexuan Zhong, Tianle Cai, Jason Lee, and Di He. REST: Retrieval-based speculative decoding. In Kevin Duh, Helena Gomez, and Steven Bethard (eds.), *Proceedings of the 2024 Conference of the North American Chapter of the Association for Computational Linguistics: Human Language Technologies (Volume 1: Long Papers)*, pp. 1582–1595, Mexico City, Mexico, 2024. Association for Computational Linguistics. URL <https://aclanthology.org/2024.naacl-long.88>.

Kaixuan Huang, Xudong Guo, and Mengdi Wang. Specdec++: Boosting speculative decoding via adaptive candidate lengths. In *Workshop on Efficient Systems for Foundation Models II@ ICML2024*, 2024.

Feiye Huo, Jianchao Tan, Kefeng Zhang, Xunliang Cai, and Shengli Sun. C2t: A classifier-based tree construction method in speculative decoding. *arXiv preprint arXiv:2502.13652*, 2025.

Sukjun Hwang, Aakash Sunil Lahoti, Ratish Puduppully, Tri Dao, and Albert Gu. Hydra: Bidirectional state space models through generalized matrix mixers. *Advances in Neural Information Processing Systems*, 37:110876–110908, 2024.

Andrei Ivanov, Nikoli Dryden, Tal Ben-Nun, Shigang Li, and Torsten Hoefler. Data movement is all you need: A case study on optimizing transformers. *Proceedings of Machine Learning and Systems*, 3:711–732, 2021.

Carlos E Jimenez, John Yang, Alexander Wettig, Shunyu Yao, Kexin Pei, Ofir Press, and Karthik R Narasimhan. SWE-bench: Can language models resolve real-world github issues? In *The Twelfth International Conference on Learning Representations*, 2024. URL <https://openreview.net/forum?id=VTF8yNQM66>.

Joao Gante. Assisted generation: a new direction toward low-latency text generation, 2023. URL <https://huggingface.co/blog/assisted-generation>.

Yaniv Leviathan, Matan Kalman, and Yossi Matias. Fast inference from transformers via speculative decoding. In Andreas Krause, Emma Brunskill, Kyunghyun Cho, Barbara Engelhardt, Sivan Sabato, and Jonathan Scarlett (eds.), *Proceedings of the 40th International Conference on Machine Learning*, volume 202 of *Proceedings of Machine Learning Research*, pp. 19274–19286. PMLR, 23–29 Jul 2023. URL <https://proceedings.mlr.press/v202/leviathan23a.html>.

Yuhui Li, Fangyun Wei, Chao Zhang, and Hongyang Zhang. Eagle-2: Faster inference of language models with dynamic draft trees. In *Proceedings of the 2024 Conference on Empirical Methods in Natural Language Processing*, pp. 7421–7432, 2024a.

Yuhui Li, Fangyun Wei, Chao Zhang, and Hongyang Zhang. EAGLE: Speculative sampling requires rethinking feature uncertainty. In Ruslan Salakhutdinov, Zico Kolter, Katherine Heller, Adrian Weller, Nuria Oliver, Jonathan Scarlett, and Felix Berkenkamp (eds.), *Proceedings of the 41st International Conference on Machine Learning*, volume 235 of *Proceedings of Machine Learning Research*, pp. 28935–28948. PMLR, 21–27 Jul 2024b. URL <https://proceedings.mlr.press/v235/1i24bt.html>.

Fangcheng Liu, Yehui Tang, Zhenhua Liu, Yunsheng Ni, Duyu Tang, Kai Han, and Yunhe Wang. Kangaroo: Lossless self-speculative decoding for accelerating LLMs via double early exiting. In *Advances in Neural Information Processing Systems*, 2024. URL <https://openreview.net/forum?id=lT3oc04mDp>.

Tianyu Liu, Yun Li, Qitan Lv, Kai Liu, Jianchen Zhu, Winston Hu, and Xiao Sun. PEARL: Parallel speculative decoding with adaptive draft length. In *The Thirteenth International Conference on Learning Representations*, 2025. URL <https://openreview.net/forum?id=Q0XrVMiHGK>.

Minh-Thang Luong, Dawsen Hwang, Hoang H Nguyen, Golnaz Ghiasi, Yuri Chervonyi, Insuk Seo, Junsu Kim, Garrett Bingham, Jonathan Lee, Swaroop Mishra, et al. Towards robust mathematical reasoning. In *Proceedings of the 2025 Conference on Empirical Methods in Natural Language Processing*, pp. 35406–35430, 2025.

Jonathan Mamou, Oren Pereg, Daniel Korat, Moshe Berchansky, Nadav Timor, Moshe Wasserblat, and Roy Schwartz. Dynamic speculation lookahead accelerates speculative decoding of large language models. In *NeurIPS Efficient Natural Language and Speech Processing Workshop*, pp. 456–467. PMLR, 2024.

Xupeng Miao, Gabriele Oliaro, Zhihao Zhang, Xinhao Cheng, Zeyu Wang, Zhengxin Zhang, Rae Ying Yee Wong, Alan Zhu, Lijie Yang, Xiaoxiang Shi, et al. Specinfer: Accelerating large language model serving with tree-based speculative inference and verification. In *Proceedings of the 29th ACM International Conference on Architectural Support for Programming Languages and Operating Systems, Volume 3*, pp. 932–949, 2024.

Ernesto Quevedo, Jorge Yero, Rachel Koerner, Pablo Rivas, and Tomas Cerny. Detecting hallucinations in large language model generation: A token probability approach. *arXiv preprint arXiv:2405.19648*, 2024.

Andrea Santilli, Silvio Severino, Emilian Postolache, Valentino Maiorca, Michele Mancusi, Riccardo Marin, and Emanuele Rodola. Accelerating transformer inference for translation via parallel decoding. In Anna Rogers, Jordan Boyd-Graber, and Naoaki Okazaki (eds.), *Proceedings of the 61st Annual Meeting of the Association for Computational Linguistics (Volume 1: Long Papers)*, pp. 12336–12355, Toronto, Canada, 2023. Association for Computational Linguistics. doi: 10.18653/v1/2023.acl-long.689. URL <https://aclanthology.org/2023.acl-long.689>.

Abigail See, Peter J Liu, and Christopher D Manning. Get to the point: Summarization with pointer-generator networks. *arXiv preprint arXiv:1704.04368*, 2017.

Noam Shazeer. Fast transformer decoding: One write-head is all you need. *arXiv preprint arXiv:1911.02150*, 2019.

Benjamin Spector and Chris Re. Accelerating llm inference with staged speculative decoding, 2023. URL <https://arxiv.org/abs/2308.04623>.

Mitchell Stern, Noam Shazeer, and Jakob Uszkoreit. Blockwise parallel decoding for deep autoregressive models. In Samy Bengio, Hanna M. Wallach, Hugo Larochelle, Kristen Grauman, Nicolò Cesa-Bianchi, and Roman Garnett (eds.), *Advances in Neural Information Processing Systems 31: Annual Conference on Neural Information Processing Systems 2018, NeurIPS 2018, December 3-8, 2018, Montréal, Canada*, pp. 10107–10116, 2018. URL <https://proceedings.neurips.cc/paper/2018/hash/c4127b9194fe8562c64dc0f5bf2c93bc-Abstract.html>.

Ziteng Sun, Ananda Theertha Suresh, Jae Hun Ro, Ahmad Beirami, Himanshu Jain, and Felix X. Yu. Spectr: Fast speculative decoding via optimal transport. In Alice Oh, Tristan Naumann, Amir Globerson, Kate Saenko, Moritz Hardt, and Sergey Levine (eds.), *Advances in Neural Information Processing Systems*, 2023. URL [http://papers.nips.cc/paper\\_files/paper/2023/hash/6034a661584af6c28fd97a6f23e56c0a-Abstract-Conference.html](http://papers.nips.cc/paper_files/paper/2023/hash/6034a661584af6c28fd97a6f23e56c0a-Abstract-Conference.html).

Hugo Touvron, Louis Martin, Kevin Stone, Peter Albert, Amjad Almahairi, Yasmine Babaei, Nikolay Bashlykov, Soumya Batra, Prajwala Bhargava, Shruti Bhosale, Dan Bikel, Lukas Blecher, Cristian Canton Ferrer, Moya Chen, Guillem Cucurull, David Esiobu, Jude Fernandes, Jeremy Fu, Wenyin Fu, Brian Fuller, Cynthia Gao, Vedanuj Goswami, Naman Goyal, Anthony Hartshorn, Saghar Hosseini, Rui Hou, Hakan Inan, Marcin Kardas, Viktor Kerkez, Madiam Khabsa, Isabel Kloumann, Artem Korenev, Punit Singh Koura, Marie-Anne Lachaux, Thibaut Lavril, Jenya Lee, Diana Liskovich, Yinghai Lu, Yuning Mao, Xavier Martinet, Todor Mihaylov, Pushkar Mishra, Igor Molybog, Yixin Nie, Andrew Poultion, Jeremy Reizenstein, Rashi Rungta, Kalyan Saladi, Alan Schelten, Ruan Silva, Eric Michael Smith, Ranjan Subramanian, Xiaoqing Ellen Tan, Bin Tang, Ross Taylor, Adina Williams, Jian Xiang Kuan, Puxin Xu, Zheng Yan, Iliyan Zarov, Yuchen Zhang, Angela Fan, Melanie Kambadur, Sharan Narang, Aurelien Rodriguez, Robert Stojnic, Sergey Edunov, and Thomas Scialom. Llama 2: Open foundation and fine-tuned chat models, 2023. URL <https://arxiv.org/abs/2307.09288>.

Simon Valentin, Jinmiao Fu, Gianluca Detommaso, Shaoyuan Xu, Giovanni Zappella, and Bryan Wang. Cost-effective hallucination detection for llms. *arXiv preprint arXiv:2407.21424*, 2024.

Jikai Wang, Yi Su, Juntao Li, Qingrong Xia, Zi Ye, Xinyu Duan, Zhefeng Wang, and Min Zhang. Opt-tree: Speculative decoding with adaptive draft tree structure. *Transactions of the Association for Computational Linguistics*, 13:188–199, 2025.

Heming Xia, Tao Ge, Peiyi Wang, Si-Qing Chen, Furu Wei, and Zhifang Sui. Speculative decoding: Exploiting speculative execution for accelerating seq2seq generation. In Houda Bouamor, Juan Pino, and Kalika Bali (eds.), *Findings of the Association for Computational Linguistics: EMNLP 2023*, pp. 3909–3925, Singapore, 2023. Association for Computational Linguistics. doi: 10.18653/v1/2023.findings-emnlp.257. URL <https://aclanthology.org/2023.findings-emnlp.257>.

Heming Xia, Zhe Yang, Qingxiu Dong, Peiyi Wang, Yongqi Li, Tao Ge, Tianyu Liu, Wenjie Li, and Zhifang Sui. Unlocking efficiency in large language model inference: A comprehensive survey of speculative decoding. In Lun-Wei Ku, Andre Martins, and Vivek Srikumar (eds.), *Findings of the Association for Computational Linguistics ACL 2024*, pp. 7655–7671, Bangkok, Thailand and virtual meeting, August 2024a. Association for Computational Linguistics. doi: 10.18653/v1/2024.findings-acl.456. URL <https://aclanthology.org/2024.findings-acl.456>.

Heming Xia, Zhe Yang, Qingxiu Dong, Peiyi Wang, Yongqi Li, Tao Ge, Tianyu Liu, Wenjie Li, and Zhifang Sui. Unlocking efficiency in large language model inference: A comprehensive survey of speculative decoding. In Lun-Wei Ku, Andre Martins, and Vivek Srikumar (eds.), *Findings of the Association for Computational Linguistics ACL 2024*, pp. 7655–7671, Bangkok, Thailand and virtual meeting, August 2024b. Association for Computational Linguistics. doi: 10.18653/v1/2024.findings-acl.456. URL <https://aclanthology.org/2024.findings-acl.456>.

Zilin Xiao, Hongming Zhang, Tao Ge, Siru Ouyang, Vicente Ordonez, and Dong Yu. ParallelSpec: Parallel draftr for efficient speculative decoding. *arXiv preprint arXiv:2410.05589*, 2024.

An Yang, Baosong Yang, Beichen Zhang, Binyuan Hui, Bo Zheng, Bowen Yu, Chengyuan Li, Dayiheng Liu, Fei Huang, Haoran Wei, et al. Qwen2. 5 technical report. *arXiv preprint arXiv:2412.15115*, 2024.

An Yang, Anfeng Li, Baosong Yang, Beichen Zhang, Binyuan Hui, Bo Zheng, Bowen Yu, Chang Gao, Chengan Huang, Chenxu Lv, et al. Qwen3 technical report. *arXiv preprint arXiv:2505.09388*, 2025.

Seongjun Yang, Gibbeum Lee, Jaewoong Cho, Dimitris Papailiopoulos, and Kangwook Lee. Predictive pipelined decoding: A compute-latency trade-off for exact LLM decoding. In *Workshop on Efficient Systems for Foundation Models @ ICML2023*, 2023. URL <https://openreview.net/forum?id=xK9FnwDMZp>.

Hanling Yi, Feng Lin, Hongbin Li, Ning Peiyang, Xiaotian Yu, and Rong Xiao. Generation meets verification: Accelerating large language model inference with smart parallel auto-correct decoding. In Lun-Wei Ku, Andre Martins, and Vivek Srikumar (eds.), *Findings of the Association for Computational Linguistics: ACL 2024*, pp. 5285–5299, Bangkok, Thailand, August 2024. Association for Computational Linguistics. doi: 10.18653/v1/2024.findings-acl.313. URL <https://aclanthology.org/2024.findings-acl.313/>.

Jun Zhang, Jue Wang, Huan Li, Lidan Shou, Ke Chen, Gang Chen, and Sharad Mehrotra. Draft& verify: Lossless large language model acceleration via self-speculative decoding. In Lun-Wei Ku, Andre Martins, and Vivek Srikumar (eds.), *Proceedings of the 62nd Annual Meeting of the Association for Computational Linguistics (Volume 1: Long Papers)*, pp. 11263–11282, Bangkok, Thailand, August 2024a. Association for Computational Linguistics. doi: 10.18653/v1/2024.acl-long.607. URL <https://aclanthology.org/2024.acl-long.607>.

Ziyin Zhang, Jiahao Xu, Tian Liang, Xingyu Chen, Zhiwei He, Rui Wang, and Zhaopeng Tu. Draft model knows when to stop: A self-verification length policy for speculative decoding. *arXiv preprint arXiv:2411.18462*, 2024b.

Weilin Zhao, Yuxiang Huang, Xu Han, Wang Xu, Chaojun Xiao, Xinrong Zhang, Yewei Fang, Kaihuo Zhang, Zhiyuan Liu, and Maosong Sun. Ouroboros: Generating longer drafts phrase by phrase for faster speculative decoding. In *Proceedings of the 2024 Conference on Empirical Methods in Natural Language Processing*, pp. 13378–13393, 2024.

Yongchao Zhou, Kaifeng Lyu, Ankit Singh Rawat, Aditya Krishna Menon, Afshin Roshtamizadeh, Sanjiv Kumar, Jean-François Kagy, and Rishabh Agarwal. DistillSpec: Improving speculative decoding via knowledge distillation. In *The Twelfth International Conference on Learning Representations*, 2024. URL <https://openreview.net/forum?id=rsY6J3ZaTF>.

## A Decoding Algorithm

---

**Algorithm 1** Speculative Decoding with PACER
 

---

**Require:** Draft model  $M_D$ , target model  $M_T$ , pre-verification layer  $M_B$ , input prefix  $\mathbf{x}$ , maximum token length  $L$ , block size  $b$ , initial threshold  $t$ , growth factor  $\rho$

```

1: while  $\text{len}(\mathbf{x}) < L$  do
2:    $\triangleright$  Adaptive draft generation
3:    $\mathbf{y}, \mathbf{q} \leftarrow [], []$   $\triangleright$  Draft tokens and Draft probabilities
4:    $i \leftarrow 1$ 
5:   while True do
6:      $(y_1, q_1, h_1), \dots, (y_b, q_b, h_b) \leftarrow M_D^b(\mathbf{x})$ 
7:      $e_1, \dots, e_b \leftarrow \text{PosEmb}(i, \dots, i + b - 1)$ 
8:      $\triangleright$  Blockwise pre-verification with past KV cache
9:      $\hat{\alpha}_1, \dots, \hat{\alpha}_b \leftarrow M_B([h_1 + e_1], \dots, [h_b + e_b])$ 
10:     $i \leftarrow i + b$ 
11:     $\mathbf{x} \leftarrow \mathbf{x} + [y_1, \dots, y_b]$ 
12:     $\mathbf{y}.\text{append}([y_1, \dots, y_b])$ 
13:     $\mathbf{q}.\text{append}([q_1, \dots, q_b])$ 
14:    if  $\text{mean}(\hat{\alpha}_1, \dots, \hat{\alpha}_b) \leq t$  then
15:      break
16:    end if
17:     $t \leftarrow t \cdot \rho$ 
18:  end while
19:   $\mathbf{x}, \mathbf{y} \leftarrow \mathbf{x}$   $\triangleright$  Split to get original input prefix
20:   $y_1, \dots, y_\gamma \leftarrow \mathbf{y}$ 
21:   $q_1, \dots, q_\gamma \leftarrow \mathbf{q}$ 
22:   $\triangleright$  Target model verification
23:   $p_1, \dots, p_{\gamma+1} \leftarrow M_T(y_1, \dots, y_\gamma; \mathbf{x})$ 
24:  Sample  $r_1, \dots, r_\gamma \sim U(0, 1)$ 
25:   $n \leftarrow \min \left( \{i - 1 \mid 1 \leq i \leq \gamma, r_i > \frac{p_i(y_i)}{q_i(y_i)}\} \cup \{\gamma\} \right)$ 
26:   $\triangleright$  Adjust target distribution if drafts are rejected
27:  if  $n < \gamma$  then
28:     $\times$  reject draft token  $y_n$ 
29:     $p' \leftarrow \text{norm}(\max(0, p_{n+1} - q_{n+1}))$ 
30:  else
31:     $\checkmark$  accept all draft tokens
32:     $p' \leftarrow p_{n+1}$ 
33:  end if
34:  Sample next token  $t \sim p'$ 
35:   $\mathbf{x} \leftarrow \mathbf{x} + [y_1, \dots, y_n, t]$ 
36: end while

```

---

## B Case Study

we provide an illustrative example comparing PACER with standard speculative decoding, as shown in Figure 4. In this example, configuration (a) uses a fixed window size of  $\gamma = 6$ , whereas configuration (b) applies PACER with a dynamic draft window and a block size of  $b = 3$ . Under the fixed-window setting, all six draft tokens are accepted in the first round; however, in the second round, all six draft tokens are rejected, resulting in unnecessary draft computation and requiring three target-model forward passes in total. In contrast, PACER halts early when draft predictions become unreliable, avoids wasted drafts, and completes the decoding process with only two target forward passes. The latency breakdown clearly demonstrates the benefit of adaptive draft control: PACER reduces total decoding time from 498.9 ms to 339.8 ms in this example, highlighting its effectiveness in lowering computational overhead and improving end-to-end efficiency.

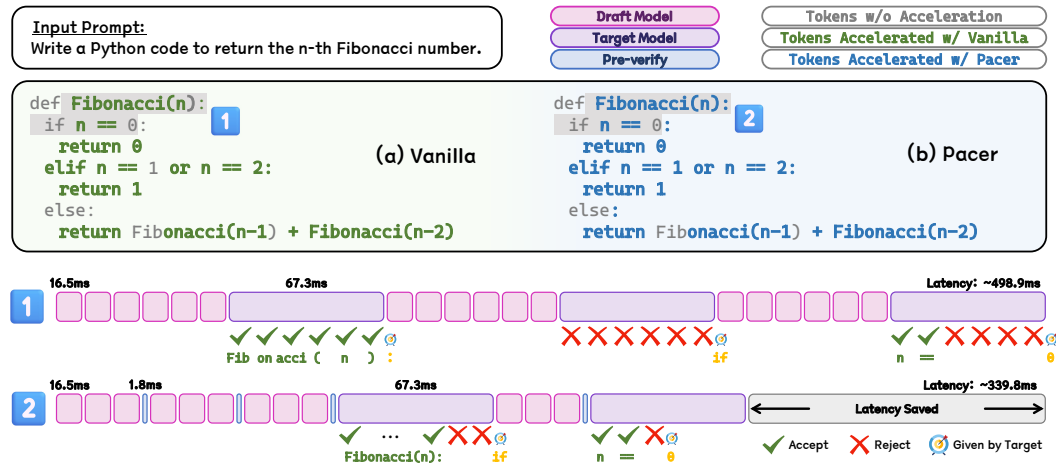


Figure 4: An illustrative comparison between vanilla SD with a fixed window size ( $\gamma = 6$ ) and PACER with a block size of  $b = 3$ . The top part of the figure shows the accelerated token generation achieved by each method. The bottom part presents a latency breakdown for generating the code snippet `Fibonacci(n): if n == 0`.

## C Experimental Details

### C.1 Evaluation Settings

**Datasets.** We evaluate our method on a range of representative text generation tasks, including HumanEval (Chen et al., 2021) and MBPP (Austin et al., 2021) for code generation, GSM8K (Cobbe et al., 2021) for arithmetic reasoning, and CNN/DailyMail (CNN/DM) (See et al., 2017) for document summarization. HumanEval comprises 164 handcrafted examples, each consisting of a text prompt and a Python function prefix. MBPP originally contains 500 diverse programming problems with corresponding test cases; we randomly sample 150 problems for evaluation. The CNN/DM dataset includes news articles paired with human-written summaries, while GSM8K features grade-school-level mathematical word problems. For both CNN/DM and GSM8K, we randomly sample 100 examples for evaluation, following (Zhao et al., 2024).

**Hardware Setting.** To validate the effectiveness of our method under both resource-constrained and resource-abundant conditions. The experiments of deepseek-coder 1.3B/33B and Qwen-2.5 1.5B/32B are performed on **1 × NVIDIA 80GB A800 GPU**, deepseek-coder 6.7B/33B on **2 × NVIDIA 80GB A800 GPU** and Llama2-chat 7B/70B on **4 × NVIDIA 80GB A800 GPU**.

**Speculative Decoding.** In Section 4, we report the performance of vanilla speculative decoding using the best decoding speed achieved across various fixed window sizes. The complete results are provided in Section F.3.

### C.2 Training Parameters

For each model series, we independently train a blockwise pre-verification layer. We use the AdamW optimizer with  $(\beta_1, \beta_2) = (0.9, 0.999)$ . All training is performed on **8 × NVIDIA A800 GPUs**. Table 9 summarizes the model scales and training configurations. The training time ranged from 18 to 47 minutes, depending on the model size.

Model Series	Pre-verification Layer Size	Learning Rate	Epochs
DeepSeek-Coder 1.3B/33B	0.18B	5e-4	5
DeepSeek-Coder 6.6B/33B	0.47B	2e-4	5
Qwen2.5 1.5B/32B	0.28B	5e-4	5
LLama2-Chat 7B/70B	0.46B	1e-4	5

Table 9: Training hyperparameters for PACER across different model series.

### C.3 Evaluation Parameters

The hyperparameters of our experiments are shown in table 10.

Task	Model	Block Size $b$	Threshold $t$	Growth Factor $\rho$
HumanEval	Deepseek 1.3B/33B	4	0.70	1.05
	Deepseek 6.7B/33B	4	0.70	1.05
	LLaMA2 7B/70B	4	0.65	1.02
MBPP	Deepseek 1.3B/33B	3	0.70	1.05
	Deepseek 6.7B/33B	3	0.70	1.05
	LLaMA2 7B/70B	3	0.70	1.05
CNN/DM	Deepseek 1.3B/33B	2	0.60	1.05
	Deepseek 6.7B/33B	2	0.60	1.05
	LLaMA2 7B/70B	3	0.65	1.05
GSM8K	Deepseek 1.3B/33B	4	0.65	1.05
	Deepseek 6.7B/33B	3	0.65	1.05
	LLaMA2 7B/70B	3	0.65	1.05

Table 10: Block size  $b$ , threshold  $t$ , and growth factor  $\rho$  used in PACER across different tasks and models in our experiments.

## D Training Details

As discussed in Section 3.3, we use the same speculative decoding (SD) process—precisely aligned with inference—to construct labeled training data. In this setup, each draft step produces a training example consisting of the input prefix and draft tokens labeled as either accepted or rejected. However, this approach is highly inefficient, as it results in approximately [Len\(dataset\)  \$\times\$  Average draft steps](#) training examples.

We observe that many draft steps share common prefixes from the same prompt and response, creating redundancy. To address this, we propose packing the training data for all draft steps corresponding to the same prompt into a single training sequence. We apply a customized attention mask during training, as illustrated in Figure 5. Specifically, the draft tokens  $d_i^i, \dots, d_i^\gamma$  represent a draft step starting from the prefix  $x_1, x_2, \dots, y_{i-1}$ , followed by  $\gamma$  sequentially generated drafts aligned to response positions  $i, \dots, \gamma$ . Each draft token  $d_i^m$  is allowed to attend only to the prefix  $x_1, x_2, \dots, y_{i-1}$  and preceding draft tokens  $d_i^i, \dots, d_i^m$ .

## E Additional Ablation Studies

We conduct additional ablation studies on block size  $b$ , threshold  $t$ , and growth factor  $\rho$  using the HumanEval dataset with DeepSeek-Coder 1.3B/33B. We report the decoding speed in tokens per second (tokens/s) for each configuration.

**Block Size  $b$ .** As shown in table 11, When the block size  $b$  is too small, the accumulation of errors may lead to premature termination of pre-verification. Conversely, when the block size  $b$  is too large, the model may fail to trigger early termination via pre-verification, resulting in unnecessary computational overhead due to generating excessive drafts.

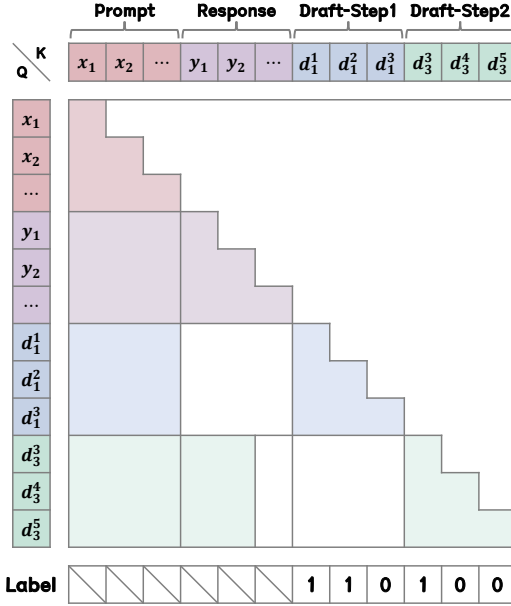


Figure 5: Customized attention mask for packing multiple draft steps into a single sequence for efficient training.

$b$	1	2	3	4	5	6	7
<b>tokens/s</b>	30.00	38.07	39.28	41.80	38.95	38.85	37.21

Table 11: Ablations on block size  $b$  where  $b \in [1, 7]$

**Growth Factor  $\rho$ .** We observe that most training examples involve shorter drafts, making it difficult for the pre-verification layer to generalize well to longer positions. In such cases, the model tends to under-predict the acceptance rate as the position grows. We conduct ablation study to demonstrate the positive effect of growth factors on decoding speed.. As show in Table 12, the heuristic growth factor (e.g., 1.05) serves as a lightweight inductive bias to encourage more aggressive drafting over time, while avoiding unbounded draft lengths.

$\rho$	1.00	1.01	1.02	1.03	1.04	1.05	1.06	1.07	1.08	1.09
<b>tokens/s</b>	40.05	40.12	40.40	40.57	40.73	41.80	41.60	40.52	39.48	39.37

Table 12: Ablations on growth factor  $\rho$  where  $\rho \in [1.00, 1.09]$

**Note.** The results for  $\rho = 1.00$  in Table 12 and for PACER w/o growth factor in the ablation study of main paper are theoretically equivalent, but differ slightly in implementation. For PACER w/o growth factor, the threshold remains constant during decoding. For Table 12 ( $\rho = 1.00$ ), the threshold is multiplied by  $\rho = 1.00$  at each step. Although this scaling should have no effect, minor discrepancies arise from subtle control flow or system-level optimizations between the two settings.

**Threshold  $t$ .** We evaluated a series of pre-verification layers under different threshold  $t$  settings, as shown in the Table 13. A threshold of 0.7 yields the best overall performance. Setting the threshold too high may lead to premature termination of pre-verification, while a threshold that is too low results in additional overhead from generating unnecessary draft tokens.

$t$	0.50	0.55	0.60	0.65	0.70	0.75	0.80
<b>tokens/s</b>	37.64	38.09	40.34	39.89	41.80	40.44	39.93

Table 13: Ablations on threshold  $t$  where  $t \in [0.50, 0.80]$ 

## F Additional Results

### F.1 Forward Latency

As shown in Table 14, the average forward-pass latencies for the blockwise pre-verification layer, draft model, and target model (DeepSeek-Coder 1.3B/33B) are 1.81 ms, 16.52 ms, and 67.31 ms, respectively. The additional overhead introduced by blockwise pre-verification is modest, approximately  $0.11 \times$  compared to the draft model and  $0.027 \times$  compared to the target model forward pass.

Model / Layer	Latency (ms)
Blockwise Pre-verification Layer	1.81
DeepSeek-Coder 1.3B	16.52
DeepSeek-Coder 33B	67.31

Table 14: Latency of a single forward pass for different model/layer in DeepSeek-Coder 1.3B/33B using PACER.

### F.2 Runtime Break of PACER

We report the actual runtime breakdown on HumanEval dataset across components for both DeepSeek-Coder 1.3B/33B and Llama-2 7B/70B models, summarized in table 15. As shown, the pre-verification layer contributes only **2.10%** and **1.30%** of the total inference time, respectively. Given the substantial speedups achieved through dynamic draft lengths (72s and 221s), this overhead is moderate in practice.

Component	DeepSeek-Coder 1.3B/33B		Llama-2 7B/70B	
	Time (s)	Portion (%)	Time (s)	Portion (%)
Pre-verification Layer	12.86	<b>2.10</b>	22.80	<b>1.30</b>
Draft Model	434.55	71.24	1080.06	61.51
Target Model	162.59	26.66	653.14	37.19
<b>Total (PACER)</b>	<b>610</b>	<b>100</b>	<b>1756</b>	<b>100</b>
Total (Speculative)	682	—	1977	—

Table 15: Time and portion analysis comparing DeepSeek-Coder and Llama-2 models.

### F.3 Detailed Results of Speculative Decoding

Model Series	1	2	3	4	5	6	7	8	9	10
DeepSeek-Coder 1.3B/33B	—	—	—	34.99	36.11	37.27	37.41	36.69	<b>37.46</b>	37.11
DeepSeek-Coder 6.7B/33B	26.83	28.81	29.35	29.57	<b>29.77</b>	29.31	29.70	29.49	29.41	—
Qwen2.5 1.5B/32B	24.07	27.29	28.14	<b>28.46</b>	27.78	27.77	27.35	26.97	26.32	—
LLama2 7B/70B	—	—	—	18.59	20.95	21.15	21.21	<b>21.23</b>	21.10	21.12

Table 16: Decoding speeds (tokens/s) for SD of various fixed window sizes ( $\gamma = 1$  to  $\gamma = 10$ ) across different model series.

For vanilla speculative decoding, we test different numbers of draft tokens as shown in Table 16, and we choose the optimal result as a baseline for our method.

#### F.4 Acceptance Rates Across Draft Positions

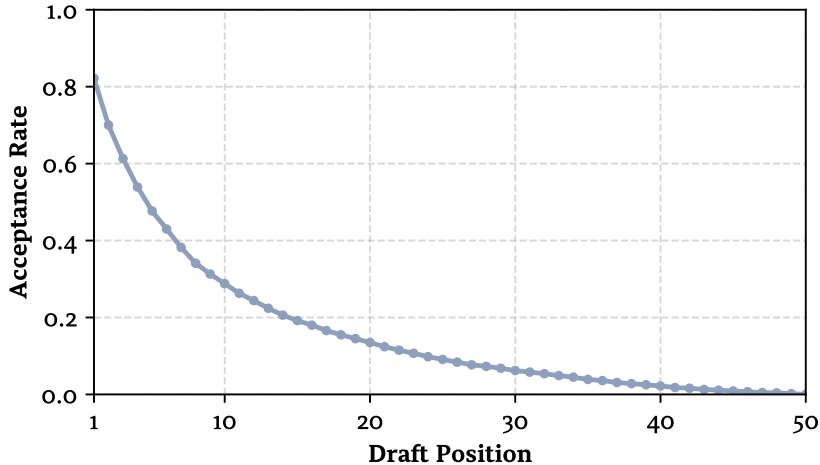


Figure 6: Acceptance rates with different draft positions.

## G Limitations

Although the proposed PACER effectively controls draft lengths dynamically and accelerates speculative decoding, it still has certain limitations. Its performance depends on the quality of drafts produced by the draft model. For tasks like code generation (e.g., HumanEval), longer average acceptance lengths yield substantial speedups; however, for summarization tasks (e.g., CNN/DM), optimal drafts tend to be shorter, limiting potential performance gains. Similarly, when both draft and target models are relatively small, the optimal draft length is short, and the relative overhead of the pre-verification layer may become more pronounced. Nevertheless, PACER complements speculative decoding techniques aimed at enhancing draft quality. Integrating PACER with Ouroboros (Zhao et al., 2024) further boosts decoding speed by up to  $3.09\times$  over autoregressive decoding. We anticipate that future research in speculative decoding will continually enhance draft quality. With such advancements, our approach is expected to achieve even more significant performance improvements.